Formation of diamonds in laser-compressed hydrocarbons at planetary interior conditions

Kraus, D.; Vorberger, J.; Pak, A.; Hartley, N. J.; Fletcher, L. B.; Frydrych, S.; Galtier, E.; Gamboa, E. J.; Gericke, D. O.; Glenzer, S. H.; Granados, E.; Macdonald, M. J.; Mackinnon, A. J.; Mcbride, E. E.; Nam, I.; Neumayer, P.; Roth, M.; Saunders, A. M.; Sun, P.; van Driel, T.; Döppner, T.; Falcone, R. W.;

Originally published:

August 2017

Nature Astronomy 1(2017), 606-611

DOI: https://doi.org/10.1038/s41550-017-0219-9

Formation of nanodiamonds in laser-compressed plastic at planetary interior conditions

D. Kraus,[1,2,3] J. Vorberger,[1] A. Pak,[4] N. J. Hartley,[1,5] L. B. Fletcher,[6] S. Frydrych,[7] E. Galtier,[6] E. J. Gamboa,[6] D. O. Gericke,[8] S. H. Glenzer,[6] E. Granados,[6] M. J. MacDonald,[6,9] A. J. MacKinnon,[6] E. E. McBride,[6,10] I. Nam,[6] P. Neumayer,[11] M. Roth,[7] A. M. Saunders,[3] P. Sun,[6] T. van Driel,[6] T. Döppner,[4] and R. W. Falcone[3,12]

[1]*Helmholtz-Zentrum Dresden-Rossendorf, Bautzner Landstrasse 400, 01328 Dresden, Germany*

[2]*Institut für Strukturphysik, Technische Universität Dresden, 01069 Dresden, Germany*

[3]*Department of Physics, University of California, Berkeley CA 94720, USA*

[4]*Lawrence Livermore National Laboratory, Livermore CA 94550, USA*

[5]*Institute for Academic Initiatives, Osaka University, Suita, Osaka 565-0871, Japan*

[6]*SLAC National Accelerator Laboratory, Menlo Park CA 94309, USA*

[7]*Institut für Kernphysik, Technische Universität Darmstadt, Schlossgartenstraße 9, 64289 Darmstadt, Germany*

[8]*Centre for Fusion, Space and Astrophysics, Department of Physics, University of Warwick, Coventry CV4 7AL, United Kingdom*

[9]*University of Michigan, Ann Arbor, Michigan 48109, USA*

[10]*European XFEL GmbH, Holzkoppel 4, 22869 Schenefeld, Germany*

[11]*GSI Helmholtzzentrum für Schwerionenforschung GmbH, Planckstraße 1, 64291 Darmstadt, Germany*

[12]*Lawrence Berkeley National Laboratory, Berkeley, California 94720, USA*

(Dated: December 13, 2016)

The effects of hydrocarbon dissociation and subsequent diamond precipitation on the internal structure and evolution of icy giant planets like Neptune and Uranus have been discussed for more than three decades[1]. Inside these celestial bodies, gravity compresses mixtures of light elements to densities of several grams per cubic centimeter while the temperature reaches thousands of Kelvins resulting in thermal energies on the order of chemical bonding and above[2]. Under these conditions, simple hydrocarbons like methane, which are highly abundant in the atmospheres of these planets[2], are believed to undergo structural transitions[3,4] that release molecular hydrogen from deeper layers and may lead to compact stratified cores[5–7]. Indeed, the isentropes of Uranus and Neptune intersect temperature-pressure conditions where first polymerization occurs[8], and then, in deeper layers, a phase separation into diamond and hydrogen may be possible. Here we show experimental evidence for this phase separation process obtained by *in situ* X-ray diffraction from polystyrene samples dynamically compressed to 150 GPa and 5000 K, which resembles the environment ∼10,000 km below the surfaces of Neptune and Uranus[9]. Our findings demonstrate the necessity of high pressures for initiating carbon-hydrogen demixing[3] and imply that diamond precipitation may require ∼10x higher pressures than previously suggested by experiments investigating non-isolated hydrocarbons[4,8,10]. Besides underlining the general importance of chemical processes inside giant planets, these results will inform evolutionary models of Uranus and Neptune, where carbon-hydrogen demixing can be a significant source for the convection necessary to explain their unusual magnetic fields[11]. Additionally, our experiment demonstrates an alternative path for producing nanodiamonds for scientific and industrial applications[12,13] that may be superior to current methods using oxygen-deficient explosives[14,15].

Being composed of highly abundant elements, hydrocarbons are one of the most common chemical species throughout the universe. A considerable share exists inside giant planets, especially icy giants like Neptune and Uranus, which are also found in steadily increasing numbers in extrasolar planetary systems. Chemical processes involving hydrocarbons can participate in shaping the interior of these planets and attempts to investigate structural transitions of such systems in the laboratory have been performed by studying methane

inside laser-heated diamond anvil cells and shock experiments with gas guns[4,10,16,17]. In diamond anvil cells, evidence for dissociation and polymerization has been found at pressures of 10-50 GPa and below the carbon melting temperature[4,10], resulting in a heavy hydrocarbon fluid[8]. Similar structural transitions are expected to happen in various hydrocarbons under shock compression[6,16,17], which first led to the postulation of possible diamond precipitation inside giant planets[1]. However, due to the lack of *in situ* measurements, details of whether, when and how diamonds can be created are not fully understood.

Some hints of diamond formation have been reported for methane samples in laser-heated diamond anvil cells at pressures of 10-50 GPa and temperatures above 2000 K (Ref. 4) or pressures of 10-80 GPa and temperatures above 3000 K (Ref. 10). Others found the appearance of carbon in form of graphite or diamond at 10-80 GPa and temperatures between 1000 K and 1500 K, but a stable fluid of heavy hydrocarbons at higher temperatures. All this is in contrast to theoretical studies with atomistic simulations, which predict that much higher pressures are required for dissociation and phase separation of hydrocarbons into diamond and hydrogen[3,18,19] ($\gtrsim$190 GPa at 2000 K and $\gtrsim$300 GPa just above 0 K). Indeed, the diamond anvil cell findings may suffer from an externally forced demixing process since atomic or molecular hydrogen is immediately absorbed by the diamond anvils[20] and the metal gasket surrounding the sample[10]. Moreover, these metal gaskets, as well as pressure standards included in the sample material, are known to significantly lower the temperature threshold for hydrocarbon dissociation[21]. The big differences between the diamond anvil cell results strongly suggest that the observed chemical reactions are mainly influenced by the specific mix of materials in contact with the sample material for each case.

In contrast, dynamic shock experiments on hydrocarbons create isolated systems while still reaching conditions similar to those investigated in diamond anvil cells. In aiming for hydrocarbon dissociation and diamond formation at higher pressures, comparable to the deeper interiors of giant planets, the difficulty is keeping the temperature below the diamond melting line due to the shock-induced entropy increase. Nevertheless, this can be achieved by using a sequence of shocks instead of a single shock, or by applying a ramp compression drive, which can result in a continuous, nearly isentropic compression[22]. Our approach employs a laser-driven two-stage shock compression of polystyrene (CH) up to pressures around 150 GPa, where the temperature is expected to remain below 6000 K. The microscopic structure is then probed *in situ* by ultrafast X-ray diffraction[23].

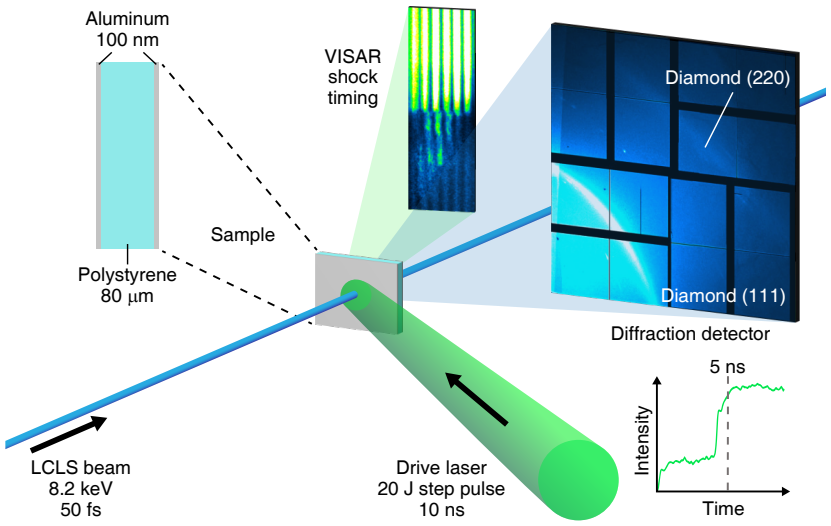

Figure 1. **Schematic of the experimental setup at the Matter at Extreme Conditions endstation of the Linac Coherent Light Source.** Two high-energy laser beams of different intensity and arrival time are overlayed to form a step pulse, which drives two shock compression waves into a polystyrene (CH) film. The shock waves are timed with a VISAR[25] to coalesce at the rear side of the sample. The microscopic state is probed by a single X-ray pulse with 8.2 keV photon energy and 50 fs pulse duration. X-ray diffraction is recorded by a large area X-ray detector, which clearly shows the formation of diamond during the second compression stage.

The experiment reported here was performed at the Matter in Extreme Conditions endstation of the Linac Coherent Light Source of Stanford National Accelerator Laboratory[24]. The available combination of high-energy lasers ($\gtrsim$10 J/pulse) with an X-ray free electron laser allows for femtosecond X-ray diffraction in order to directly access the kinetics of shock-induced structural transitions. A schematic of the experiment is shown in Fig. 1. The polystyrene sample is compressed by a step pulse laser profile that had been adjusted for optimal sample conditions using a Velocity Interferometer System for Any Reflector (VISAR)[25] (see Methods section). The initial drive intensity of 2.7×10^{12} W/cm^2 lasts for 4.5 ns before being raised to 7.1×10^{12} W/cm^2. This results in two stages of shock compression that create conditions similar to planetary interiors at 150 GPa. A single shock compression producing the same final pressure would instead lead to temperatures well above the melting line of diamond and higher than predicted in the interior of the icy giants in our solar system.

One-dimensional hydrodynamic simulations of the two-step shock compression using

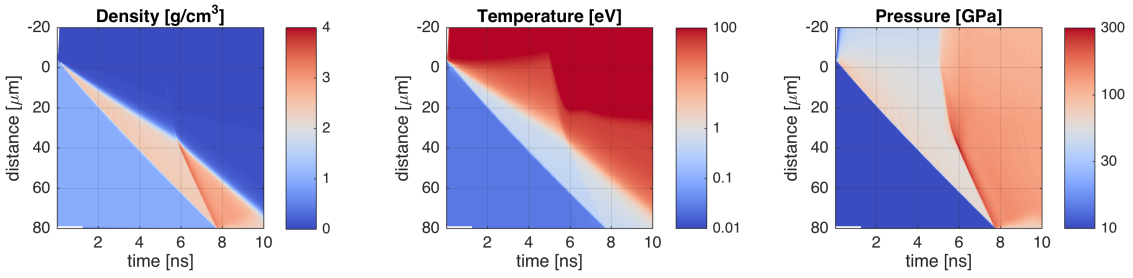

Figure 2. **Hydrodynamic simulations of the two-stage shock compression.** The drive laser hits the sample from the top in all diagrams and the double-stage drive results in two time-delayed shock compression waves. The second shock enters the sample ∼6 ns after the first compression wave and both shocks coalesce at 7.5 ns when reaching the sample rear side at d=80µm. At this time, relatively homogeneous conditions of ρ=3 g/cm^3, T=5000 K and P=150 GPa are predicted in the compressed sample material.

HELIOS[26] are illustrated in Fig. 2. The drive intensity used in the simulations is adjusted to the shock timing measured in the experiment. The first shock has a transit time of 7.5 ns while the second forms when the drive laser reaches maximum intensity and enters the pre-shocked dense material ∼6 ns after the start of the laser drive. The two shocks then coalesce at the rear side 1.5 ns later. Using the SESAME 7590 equation of state for polystyrene, which gives a good fit to Hugoniot and brightness temperature measurements in this regime[27], we obtain a density of 3.0 g/cm^3, a temperature of 5000 K and a pressure of 150 GPa as average conditions in the double-shocked material. This closely resembles the predicted environment at ∼10,000 km into the interiors of Neptune or Uranus[2,9].

Lineouts of *in situ* X-ray diffraction at various time delays are shown in Fig. 3. At ambient conditions, clear signatures of the amorphous polystyrene are observed together with various weak Bragg reflections from the aluminum coating on both sides. When launching the shock wave into the sample, half of the aluminum coating immediately vanishes as the front layer is vaporized and ablated by the laser drive. At the same time, the ambient amorphous diffraction features start to decrease as the compression waves travel through the sample. In good agreement with the hydrodynamic simulations, which predict that the second shock enters the dense pre-shocked material 6 ns after the start of the laser drive, we find the onset of new diffraction features at 6.2 ns. These peaks are compatible with the (111) and (220) Bragg reflections of compressed diamond at a density of 4.1 g/cm^3 and grow until 7.4 ns,

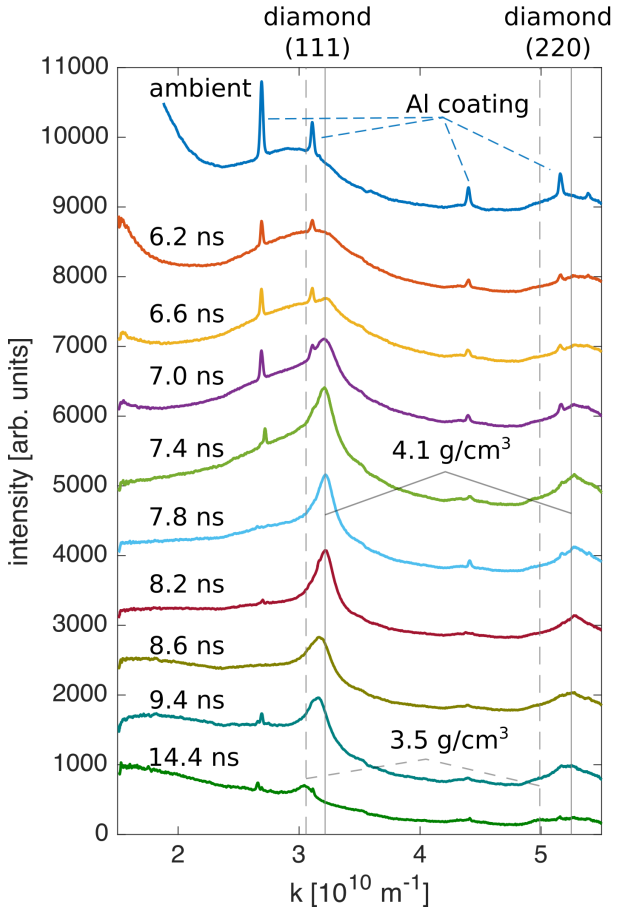

Figure 3. **Diffraction lineouts.** The diffraction signals of cold undriven samples show the typical features of amorphous polystyrene together with Bragg reflections from the aluminum coatings on the front and rear side. After the second shock wave has entered the pre-compressed sample, a strong diffraction signature of compressed diamond starts to appear. This feature remains after the shock release and shows decompression of the nanodiamonds to ambient density.

when the two shock fronts reach the rear surface. The width of the diffraction allows for inferring a lower limit of the nanodiamond particle size via the Scherrer formula[28]. We find a FWHM of $0.17\,\text{Å}^{-1}$ (2.9 degrees) for the (111) reflection, which implies nanodiamonds of at least 4 nm in diameter. We do not observe any signature of diamond when just applying a single shock compression drive (shock pressures between 50 GPa and 180 GPa have been applied to the sample). In this case, the compressed polystyrene remains in an amorphous, complex liquid[29] or dense plasma state.

Fig. 4 compares our results to planetary models, atomistic simulations of the carbon-hydrogen phase separation and previous experiments with diamond anvil cells. We do not

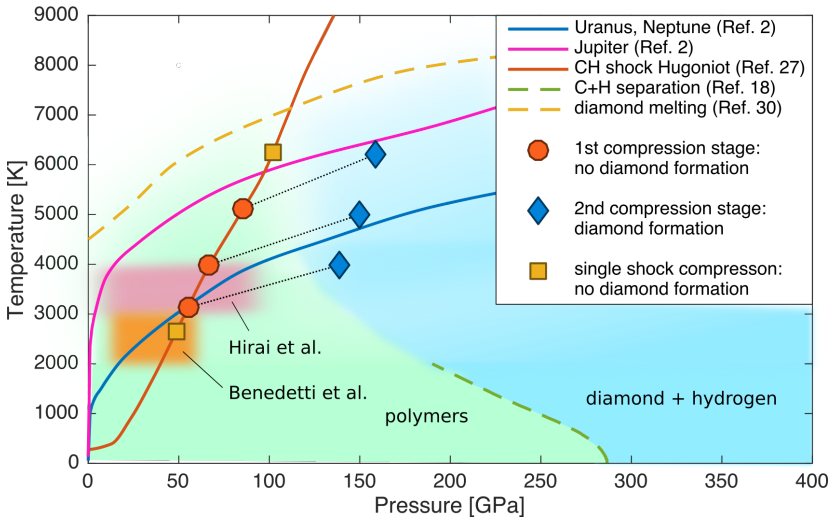

Figure 4. **Summary of the results.** We observe diamond formation around 150 GPa and 5000 K, which overlaps with the predicted isentropes of Uranus and Neptune[2]. At the same time no trace of diamond is found when applying a single shock on polystyrene, which intersects the regime where diamond formation was suggested by experiments in diamond anvil cells (Benedetti et al., Ref. 4 and Hirai et al., Ref. 10). This supports the trend given by atomistic simulations, which predict the phase separation only at higher pressures.

observe any evidence of diamond formation on the probed section of the polystyrene shock Hugoniot curve, which overlaps with the region of the phase diagram covered by experiments with diamond anvil cells. Moreover, we do not find that diamond formation mainly scales with temperature above a pressure threshold of ∼10 GPa, as reported in Ref. 10. Instead, in our experiment, diamond is only observed after compression by the second shock wave. Diamond is also produced when slightly varying the laser intensity of the two compression stages (1.7×10^{12} W/cm^2 followed by 6.4×10^{12} W/cm^2 and 3.2×10^{12} W/cm^2 followed by 8.0×10^{12} W/cm^2 were applied). This leads to reduced or increased pressure/temperature conditions: 139 GPa, 4200 K and 159 GPa, 6100 K according to the described hydrodynamic simulations that were benchmarked by the recorded shock timings. In all cases, the second shock raises the pressure by a factor of 2-3, but increases the temperature by only ∼20%. This pressure dependence is more in line with atomistic modeling and therefore suggests that the non-isolated nature of samples tested in diamond anvil cells may obscure conclusions about the carbon-hydrogen phase separation inside planets. In general, our results

support the idea of carbon-hydrogen demixing and subsequent diamond precipitation inside hydrocarbon-bearing giant planets, where the temperature remains below the diamond melting line[30], but imply that it probably requires higher pressures than suggested by previous experimental work. It needs to be pointed out that the timescales of diamond anvil cell experiments (seconds) are very different to dynamic laser compression experiments (nanoseconds) and both experimental methods are certainly far off quantum molecular dynamics simulations (picoseconds) as well as planetary time scales (millions of years). Therefore, future experiments should aim to obtain precise information on the kinetics of the demixing and phase separation processes in order to achieve extrapolations that can fully constrain models for the internal structure and evolution of giant planets.

In addition to their relevance for planetary modelling, by showing the formation and release of nanodiamonds, our results identify a possible method to produce nanodiamonds from plastics for scientific and industrial applications. The occurrence of so-called detonation nanodiamonds in the soot of oxygen-deficient explosives has been known since the 1960s[14,15] and, since the 1990s, this method has been applied as a commercial source of nanodiamonds, which show a steadily increasing number of scientific and industrial applications[12,13]. Very similar diamond nanoparticles are evidently created in our laser-driven polystyrene samples. In fact, high-repetition rate laser systems (10 Hz or more) with comparable pulse energy as used for our measurements are nowadays readily available and the required double-stage shock compression can simply be realized by using two time-delayed drive lasers (as demonstrated in our experiment). Such laser irradiation of fast moving plastic films above a cooling medium like water could be a cleaner, easier to control and thus eventually cheaper method than the current industrial nanodiamond production using explosives.

METHODS

Laser-driven double-stage shock compression

The samples were laser-cut out of a high-purity polystyrene film (ρ_0=1.046 g cm^{-3}, 83.4 µm thick) and compressed using two pulsed high-energy lasers (527 nm, 10 ns pulse duration, 200 µm focal spot diameter, smoothed with random phase plates). The two beams were set to different pulse energies and timing with respect to the X-ray probe in

order to create the desired two-stage shock compression drive. The laser pulse striking the sample first was set to an energy of 8 J, the subsequent pulse reached its maximum intensity 5 ns after the initial pulse and its energy was set to 16 J. The two resulting shock waves were timed with the VISAR system using samples with single-crystal lithium fluoride (LiF) windows at the rear side. With this method, the plastic/LiF interface velocity could be monitored at the moment when a shock front reaches the rear side of the plastic samples. A relatively low interface velocity thus implies that the initial shock reaches the rear side first, whereas a high velocity is clearly connected with the stronger shock overtaking the initial wave before reaching the sample rear side. Adjusting the relative timing and pulse energy of the laser pulses to the values mentioned above ensured shock coalescence very close to the plastic sample rear side. In this way, a reasonably homogeneous sample can be probed by the X-rays at the moment when both shocks reach the rear side. The other described drives were realized with 6 J or 11.5 J in the first pulse and again 16 J in the second pulse. In these cases, the shocks are not optimally timed to coalesce at the rear side, however, clear diamond formation is also recorded starting at the instance when the second shock is expected to enter the dense pre-shocked material. Without the LiF window at the rear side, the VISAR just records a strong drop in reflectivity, but no fringe shift due to rapid evaporation and disassembly of the reflective 100 nm thick aluminum coating. However, during the X-ray shots, the LiF windows were not applied in order to avoid obscuring diffraction signals as well as damage to the X-ray detectors due to strong single crystal reflections. The spatial resolution of the VISAR diagnostic also allows for assessing planarity and the steadiness of the shock waves. We find a planar shock release at the sample rear side in a 50 µm window. Moreover, the polystyrene/LiF interface velocity remains constant within the planar region of the shock release for several ns, which implies reasonably steady shocks. The arrival time of the drive laser was determined by the same streak cameras as used for the VISAR system by scattering light of the drive laser beams from the exact position of sample interaction into the VISAR system.

Ultrafast X-ray diffraction

The polystyrene samples were probed using the LCLS XFEL beam in SASE mode (8.2 keV photon energy, 0.3 % spectral bandwidth, 50 fs pulse duration, 20 µm spot size, ∼3 mJ per

pulse corresponding to 2×10^{12} photons per pulse). Using imprints of the X-rays in the aluminum coating on the sample rear side that is monitored by the VISAR diagnostic, an accuracy of 20 µm or better could be achieved for the spatial overlap of X-rays and the drive lasers. The timing of the X-ray pulse relative to the drive laser was chosen to probe the sample slightly before or exactly at the moment when the shock waves coalesce at the end of the plastic samples. X-ray diffraction was measured by an 8x8 cm^2 Cornell-Stanford Pixel Array detector (CSPAD) at 8.7 cm distance from the sample covering diffraction angles from 18 to 85 degrees above the XFEL beam axis. In this way, perturbing effects due to the horizontal polarization of the X-ray beam could be avoided. Angular calibration for the recorded 2θ range was obtained by diffraction of CeO_2 and LaB_6 powder samples.

[1] Ross, M. The ice layer in Uranus and Neptune-diamonds in the sky? *Nature* **292,** 435 (1981).

[2] Guillot, T. Interiors of Giant Planets Inside and Outside the Solar System. *Science* **286,** 72 (1999).

[3] Ancilotto, F., Chiarotti, G. L., Scandolo, S. & Tosatti, E. Dissociation of Methane into Hydrocarbons at Extreme (Planetary) Pressure and Temperature. *Science* **275,** 1288 (1997).

[4] Benedetti, L. R., Nguyen, J. H., Caldwell, W. A., Liu, H., Kruger & Jeanloz, R. Dissociation of CH_4 at High Pressures and Temperatures: Diamond Formation in Giant Planet Interiors? *Science* **100,** 1288 (1999).

[5] Hubbard, W. B., Nellis, W. J., Mitchell, A. C., Limaye, S. S. & McCandless, P. C. Interior Structure of Neptune: Comparison with Uranus. *Science* **253,** 648 (1991).

[6] Chau, R., Hamel, S. & Nellis, W. J. Chemical processes in the deep interior of Uranus. *Nat. Commun.* **2,** 203 (2011).

[7] Nettelmann, N., K. Wang, K., Fortney, J. J., Hamel, S., Yellamilli, S., Bethkenhagen, M., & Redmer, R. Uranus evolution models with simple thermal boundary layers. *Icarus* **275,** 107 (2016).

[8] Lobanov, S. S, Chen, P.-N., Chen, X.-J., Zha, C.-S., Litasov, K. D., Mao, H.-K. & Goncharov, A. F. Carbon precipitation from heavy hydrocarbon fluid in deep planetary interiors. *Nat. Commun.* **4,** 2446 (2013).

[9] Helled, R., Anderson, J. D., Podolak, M. &Schubert, G. Interior models of Uranus and Neptune. *Astrophys. J.* **7,** 15 (2011).

[10] Hirai, H., Konagai, K., Kawamurab, T., Yamamotob, Y. & Yagic, T. Polymerization and diamond formation from melting methane and their implications in ice layer of giant planets. *Physics of the Earth and Planetary Interiors* **174,** 242 (2009).

[11] Stanley, S. & Bloxham, J. Convective-region geometry as the cause of Uranus' and Neptune's unusual magnetic fields. *Nature* **428,** 11 (2004).

[12] Maze, J. R. *et al.* Nanoscale magnetic sensing with an individual electronic spin in diamond. *Nature* **455,** 644-647 (2008).

[13] Vaijayanthimala, V. & Chang, H. C. Functionalized fluorescent nanodiamonds for biomedical applications. *Nanomedicine* **4,** 47-55 (2009).

[14] Mochalin, V. N., Shenderova, O., Ho, D. & Gogotsi, Y. The properties and applications of nanodiamonds. *Nat. Nanotechnology* **7,** 11 (2012).

[15] Greiner, N. R., Phillips, D. S., Johnson, J. D. & Volk, F. Diamonds in detonation soot. *Nature* **333,** 440 (1988).

[16] Nellis, W. J., Ree, F. H., van Thiel, M. & Mitchell, A. C. Shock compression of liquid carbon monoxide and methane to 90 GPa (900 kbar) *J. Chem. Phys.* **75,** 3055 (1981).

[17] Nellis, W. J., Hamilton, D. C. & Mitchell, A. C. Electrical conductivities of methane, benzene, and polybutene shock compressed to 60 GPa (600 kbar). *J. Chem. Phys.* **115,** 1015 (2001).

[18] Gao, G., Oganov, A. R., Ma, Y., Wang, H., Li, P., Li, Y., Iitaka, T. & Zou, G. Dissociation of methane under high pressure. *J. Chem. Phys.* **133,** 144508 (2010).

[19] Sherman, B. L., Wilson, H. F., Weeraratne, D. & Militzer, B. Ab initio simulations of hot dense methane during shock experiments. *Phys. Rev. B 86,* 224113 (2012).

[20] Uzan-Saguy, C. *et al.* Diffusion of hydrogen from a microwave plasma into diamond and its interaction with dopants and defects. *Diamond and Related Materials* **11,** 316-322 (2002).

[21] Ahmed, S. Abdullah, A., Rahman, F., Al-Dawood, A., & Al-Muhaish, F. Decomposition of hydrocarbons to hydrogen and carbon. *Applied Catalysis A: General*, **359,** 1-24 (2009).

[22] Smith, R. F. *et al.* Ramp compression of diamond to five terapascals. *Nature* **511,** 330 (2014).

[23] Kraus, D. *et al.* Nanosecond formation of diamond and lonsdaleite by shock compression of graphite. *Nat. Commun.* **7,** 10970 (2016).

[24] Glenzer, S. H. *et al.* Matter under extreme conditions experiments at the Linac Coherent Light Source. *J. Phys. B: At. Mol. Opt. Phys.* **49,** 092001 (2016).

[25] Barker, L. M. & Hollenbach, R. E. Laser interferometer for measuring high velocities of any reflecting surface. *J. Appl. Phys.* **43,** 4669 (1972).

[26] MacFarlane, J. J., Golovkin, I. E. & Woodruff, P. R. HELIOS-CR - A 1-D radiation-magnetohydrodynamics code with inline atomic kinetics modeling. *J. Quant. Spectrosc. Rad. Transfer* **99**, 381 (2006).

[27] Barrios, M. A., Hicks, D. G., Boehly, T. R., Fratanduono, D. E., Eggert, J. H., Celliers, P. M., Collins, G. W. & Meyerhofer, D. D. High-precision measurements of the equation of state of hydrocarbons at 1-10 Mbar using laser-driven shock waves. *Phys. Plasmas* **17,** 056307 (2010).

[28] Scherrer, P. Bestimmung der Größe und der inneren Struktur von Kolloidteilchen mittels Röntgenstrahlen. *Göttinger Nachrichten* **2,** 98 (1918).

[29] Kraus, D. *et al.*, Probing the Complex Ion Structure in Liquid Carbon at 100 GPa. *Phys. Rev. Lett.* **111,** 255501 (2013).

[30] Wang, X., Scandolo, S. & Car, R. Carbon Phase Diagram from Ab Initio Molecular Dynamics. *Phys. Rev. Lett.* **95,** 185701 (2005).

ACKNOWLEDGMENTS

This work was performed at the Matter at Extreme Conditions (MEC) instrument of LCLS, supported by the U. S. Department of Energy Office of Science, Fusion Energy Science under contract No. SF00515. D.K., A.M.S., and R.W.F acknowledge support by the U.S. Department of Energy, Office of Science, Office of Fusion Energy Sciences and by the National Nuclear Security Administration under Award Numbers DE-FG52-10NA29649 and DE-NA0001859. D.K. and N.J.H. were supported by the Helmholtz Association under VH-NG-1141. SLAC HED is supported by DOE Office of Science, Fusion Energy Science under FWP 100182. S.F. and M.R. were supported by German Bundesministerium für Bildung und Forschung project No. 05P15RDFA1. The work of A.P. and T.D. was performed under the auspices of the U.S. Department of Energy by Lawrence Livermore National Laboratory under Contract No. DE-AC52-07NA27344.

AUTHOR CONTRIBUTIONS

D.K., R.W.F., J.V., T.D., A.P., S.H.G., D.O.G., M.R., E.Ga., E.Gr., P.N. and A.J.M. were involved in the project planning. D.K., E.Ga., N.J.H., A.P., T.D., P.N., E.E.M., A.M.S., S.F., L.B.F., P.S., M.J.M., E.J.G., E.Gr., I.N. and T.v.D. carried out the experiment. Experimental data was analyzed and discussed by D.K., J.V., N.J.H., S.H.G., D.O.G., A.P., E.E.M. and T.D. The manuscript was written by D.K., J.V., A.P., N.J.H., M.J.M, D.O.G. and T.D.

ADDITIONAL INFORMATION

The authors declare that there are no competing financial interests. Correspondence and requests for material should be addressed to D.K. (d.kraus@hzdr.de).